Iranian Journal of Electrical and Electronic Engineering 04 (2020) 551–558

IUST Iran University of Science and Technology

Iranian Journal of Electrical and Electronic Engineering

Journal Homepage: ijeee.iust.ac.ir

Research Paper

# Lyapunov-Based Robust Power Controllers for a Doubly Fed Induction Generator

Y. Djeriri*(C.A.)

**Abstract:** In this work, a robust nonlinear control technique of a doubly fed induction generator (DFIG) intended for wind energy systems has been proposed. The principal idea in this article is to decouple the active and reactive power of the DFIG with high robustness using the backstepping strategy. The principle of this control method is based on the Lyapunov function, in order to guarantee the global asymptotic stability of the system. Finally, we present some simulation results in order to verify the efficiency and robustness of the proposed control technique.

**Keywords:** DFIG, Nonlinear Control, Backstepping, Robustness, Lyapunov Function.

## 1 Introduction

WIND energy is one of the largest and most promising sources of renewable energy in the world in terms of development, because it is non-polluting and economically viable. Institutional and government support, together with the high wind energy potential and the development of energy conversion technologies, has enabled a fast development of wind energy with an increment rate of 30% worldwide [1].

Currently, the wind turbine generators market with variable speed has turned to powers greater than 1MW in particular to make the most of the wind farm on the site of implantation. These generators often use the doubly fed induction machine as a generator because of its advantages. In fact, the most typical connection diagram of this machine is to connect the stator directly to the grid, while the rotor is fed through two static converters in back-to-back mode (one RSC at the rotor side and the other at the grid side GSC). This last configuration allows the variable speed operation of wind turbine, which gives the possibility of producing the maximum possible power over a wide range of speed variation (±30% near the synchronous speed). In addition, the static converters used for the control of this machine can be sized to pass only a fraction of the total power (which represents the power of the slip). This implies fewer commutative losses, a lower conversion cost of the converter and a reduction in the size of the passive filter, thus reducing costs and additional losses [2, 3].

Traditionally, vector control based on conventional Proportional-Integral (PI) controllers is introduced to the power control of the DFIG, which decouples DFIG active and reactive powers, and reaches good performances in the wind energy systems [4]. However, the classical PI controller may not give satisfactory performances against parameters variations of the system [4, 5].

Recently, several nonlinear control laws based a DFIG are presented in literature such as feedback linearizing control technique [6], sliding mode control method [7]

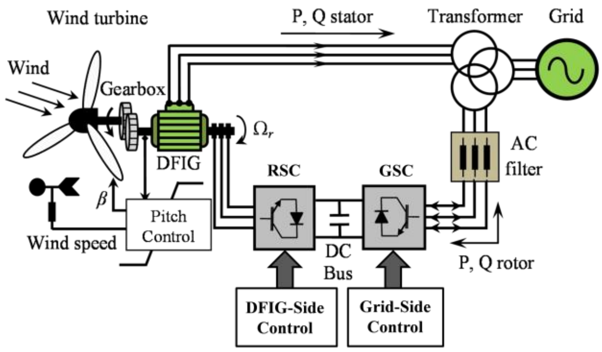


**Fig. 1** WES-based a DFIG configuration.

Iranian Journal of Electrical and Electronic Engineering, 2020.
Paper first received 18 September 2019, revised 05 February 2020, and accepted 11 February 2020.
* The author is with the Intelligent Control and Electrical Power Systems Laboratory, Faculty of Electrical Engineering, Djillali Liabes University, PO Box 89, Sidi Bel-Abbes, 22000, Algeria.
E-mail: youcef.djeriri@univ-sba.dz.
Corresponding Author: Y. Djeriri.

and backstepping control strategy [8], etc. This paper discusses synthesis of a backstepping algorithm for the control of a DFIG associated with a wind turbine. This control strategy is applied to the rotor side converter (RSC) in the wide range of speed variation of DFIG; it allows a direct power control without inner current control loops contrary to [8]. This technique is based on the use of the Lyapunov function, which facilitates the study of stability [9].

## 2 Wind Turbine Model

In this study, we have represented the evolution of the wind speed, by a scalar function that evolves over time, modeled in deterministic form by a sum of several harmonics as follows:

$$\begin{aligned} v(t) &= 8.2 + 2\sin(\omega t) - 1.75\sin(3\omega t) + 1.5\sin(5\omega t) \\ &\quad -1.25\sin(10\omega t) + \sin(30\omega t) + 0.5\sin(50\omega t) \\ &\quad +0.25(100\,\omega t) \end{aligned} \tag{1}$$

where $\omega = 2\pi/10$.

The wind speed profile modeled by (1) is illustrated in Fig. 2.

The aerodynamic power of the wind turbine can be given as follows:

$$P_t = \frac{1}{2}\rho\,\pi R^2 v^3 C_p(\lambda,\beta) \tag{2}$$

where

$$\lambda = \frac{\Omega_r R}{v} \tag{3}$$

The power coefficient can be expressed by the following expression:

$$C_p = C_1\left(\frac{C_2}{\lambda_i} - C_3\beta - C_4\right)\exp\left(\frac{-C_5}{\lambda_i}\right) + C_6\lambda \tag{4}$$

where

$$\frac{1}{\lambda_i} = \frac{1}{\lambda + 0.08\beta} - \frac{0.035}{\beta^3 + 1} \tag{5}$$

The expression of the aerodynamic torque of the turbine can be determined as follows:

$$T_t = \frac{P_t}{\Omega_r} = \frac{1}{2}\rho\,\pi R^3 v^2 C_t(\lambda,\beta) \tag{6}$$

The torque coefficient $C_t$ is defined by:

$$C_t = \frac{C_p}{\lambda} \tag{7}$$

Fig. 3 shows power coefficient $C_p$ curves as a function of the tip-speed ratio $\lambda$ for different pitch angles $\beta$.

## 3 Maximum Power Point Tracking Technique Design

In order to realize the MPPT control, it is necessary to estimate the reference speed of the generator [10]. To do that, we use the Eq.3, the speed reference $\Omega_g$* can be given by:

$$\Omega_g^* = \frac{\lambda_{opt}\, v\, G}{R} \tag{8}$$

This estimated speed is compared with the real DFIG speed in order to generate the reference DFIG torque via a PI controller. Fig. 4 shows the closed-loop speed for the MPPT technique.

By using poles placement method, the two PI controller adjustment gains ($K_p$ and $K_i$) are given by:

$$\begin{cases} K_i = \omega_n^2 J \\ K_p = 2\xi J\,\omega_n - f_r \end{cases} \tag{9}$$

where $\xi$ is the damping ratio, $\omega_n$ is the undamped natural frequency, and for $\xi = 1$ and $\omega_n = 100$ rad/s, the values of $K_p$ and $K_i$ are given in the Appendix.

The MPPT technique based PI controller has, as shown in Fig. 5, kept the power coefficient $C_p$ at its

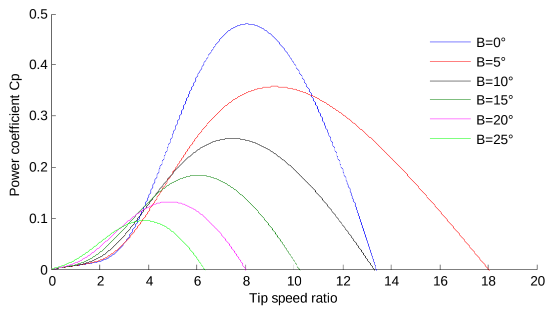


**Fig. 3** Power coefficient curves.

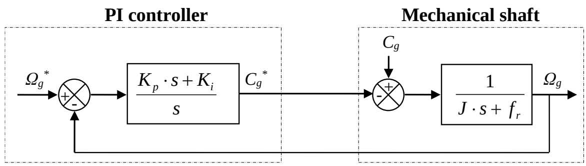


**Fig. 4** Block diagram of the speed control loop for the MPPT algorithm.

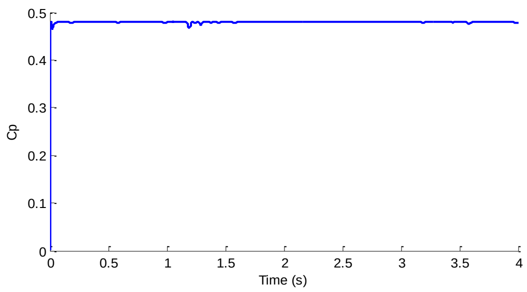


**Fig. 5** Maximum power coefficient achieved by MPPT control technique.

maximum value ($C_{pmax}$=0.48) which corresponds for an optimal tip-speed ratio ($\lambda_{opt}$=8.1). We take note that the blades orientation angle is fixed $\beta = 0$.

## 4 Mathematical Model of DFIG

We can model the DFIG in the d-q frame linked to the rotating field by the following equation system:
Stator voltage components:

$$\begin{cases} V_{ds} = R_s I_{ds} + \dfrac{d}{dt}\psi_{ds} - \omega_s \psi_{qs} \\ V_{qs} = R_s I_{qs} + \dfrac{d}{dt}\psi_{qs} + \omega_s \psi_{ds} \end{cases} \tag{10}$$

Rotor voltage components:

$$\begin{cases} V_{dr} = R_r I_{dr} + \dfrac{d}{dt}\psi_{dr} - (\omega_s - \omega_r)\psi_{qr} \\ V_{qr} = R_r I_{qr} + \dfrac{d}{dt}\psi_{qr} + (\omega_s - \omega_r)\psi_{dr} \end{cases} \tag{11}$$

Stator flux components:

$$\begin{cases} \psi_{ds} = L_s I_{ds} + L_m I_{dr} \\ \psi_{qs} = L_s I_{qs} + L_m I_{qr} \end{cases} \tag{12}$$

Rotor flux components:

$$\begin{cases} \psi_{dr} = L_r I_{dr} + L_m I_{ds} \\ \psi_{qr} = L_r I_{qr} + L_m I_{qs} \end{cases} \tag{13}$$

DFIG electromagnetic torque:

$$T_{em} = \frac{3}{2} p \frac{L_m}{L_s}\left(\psi_{qs} I_{dr} - \psi_{ds} I_{qr}\right) \tag{14}$$

Mechanical equation:

$$T_t = T_{em} + J\frac{d\Omega_r}{dt} + f_r \Omega_r \tag{15}$$

The stator powers are expressed by:

$$\begin{cases} P_s = \dfrac{3}{2}\left(V_{ds} I_{ds} + V_{qs} I_{qs}\right) \\ Q_s = \dfrac{3}{2}\left(V_{qs} I_{ds} - V_{ds} I_{qs}\right) \end{cases} \tag{16}$$

To simplify the DFIG model, the orientation of the stator flux on the $d$-axis of the Park frame was used, as shown in Fig. 6.

For medium and large power machines, the stator resistance can be neglected [11]. Consequently:

$$\begin{cases} \psi_{ds} = \psi_s \\ \psi_{qs} = 0 \end{cases} \tag{17}$$

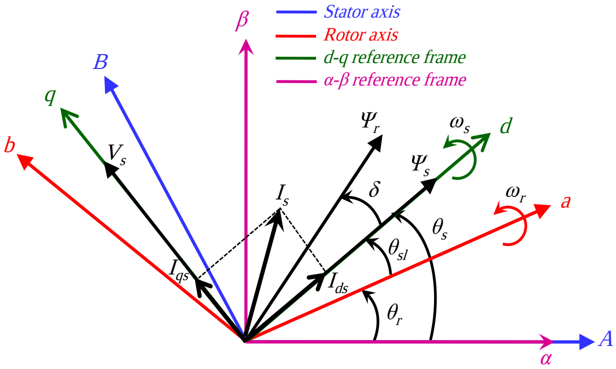


**Fig. 6** Stator field oriented control technique.

We consider that the wind turbine is connected to a powerful and stable grid, and we also neglect the drop voltage in the stator resistance [11, 12], the mathematical model of the DFIG can be simplified as follows:

$$\begin{cases} V_{ds} = 0 \\ V_{qs} = V_s = \omega_s \psi_s \end{cases} \tag{18}$$

$$\begin{cases} \psi_s = L_s I_{ds} + L_m I_{dr} \\ 0 = L_s I_{qs} + L_m I_{qr} \end{cases} \tag{19}$$

$$\begin{cases} I_{ds} = \dfrac{\psi_s}{L_s} - \dfrac{L_m}{L_s} I_{dr} \\ I_{qs} = -\dfrac{L_m}{L_s} I_{qr} \end{cases} \tag{20}$$

$$\begin{cases} P_s = \dfrac{3}{2} V_s I_{qs} \\ Q_s = \dfrac{3}{2} V_s I_{ds} \end{cases} \tag{21}$$

By substituting (20) in (21), the stator active and reactive powers are expressed by:

$$\begin{cases} P_s = -\dfrac{3}{2}\dfrac{L_m}{L_s} V_s I_{qr} \\ Q_s = \dfrac{3}{2} V_s \left(\dfrac{V_s}{L_s\,\omega_s} - \dfrac{L_m}{L_s} I_{dr}\right) \end{cases} \tag{22}$$

The electromagnetic torque is as follows:

$$T_{em} = -\frac{3}{2} p \frac{L_m}{L_s} \psi_s I_{qr} \tag{23}$$

## 5 Backstepping Control of DFIG

### 5.1 Backstepping Control Principle

During the last years, many non-linear control techniques have been proposed. The backstepping technique is one of the most popular techniques in the literature [13-15]. It proposes an essential method of synthesis towards the class of nonlinear systems having a triangular form. It is based on the decomposition of the entire control system, which is usually multivariable (MIMO) and high order into a cascade of first-order sub-control systems. The basic idea of the backstepping technique is to recursively choose some appropriate state functions like virtual control inputs for first-order subsystems of the global system [16]. The determination of the control laws that follows from this approach is based on the use of Control Lyapunov Functions (CLF) [8, 17]. In this study, we use only two backstepping controllers to control directly the active and the reactive power of the DFIG, in contrary to [8, 10, 14] and [16-18], who use more than two controllers (three or four controllers).

### 5.2 Backstepping Controllers Design

The main objective of using the backstepping technique in this paper is to control directly and independently the stator powers of the DFIG via the RSC of the latter.

The design of the backstepping controller can be attained in two steps [13]:

**A) Active Power Control**

The active power error can be given by:

$$e_1 = P_s^* - P_s \tag{24}$$

The derivative of (24) is:

$$\dot{e}_1 = \dot{P}_s^* - \dot{P}_s \tag{25}$$

Considering $V$ as a Lyapunov candidate function:

$$V(e_1) = \frac{1}{2}e_1^2 \tag{26}$$

The derivative of (26) is given by:

$$\dot{V}(e_1) = e_1\dot{e}_1 = e_1\left(\dot{P}_s^* - \dot{P}_s\right) \tag{27}$$

Replacing (22) in (27), we obtain:

$$\dot{V}(e_1) = e_1\left(\dot{P}_s^* + \frac{3}{2}\frac{L_m}{L_s}V_s\dot{I}_{qr}\right) \tag{28}$$

Such as the derivative of $I_{qr}$ is given as follows:

$$\dot{I}_{qr} = \frac{dI_{qr}}{dt} = -g\,\omega_s I_{dr} - \frac{R_r}{\sigma L_r}I_{qr} - \frac{g\,L_m V_s}{\sigma L_s L_r} + \frac{V_{qr}}{\sigma L_r} \tag{29}$$

Equation (28) becomes:

$$\dot{V}(e_1) = e_1\left(\dot{P}_s^* + \frac{3}{2}\frac{L_m}{L_s}V\left(-g\,\omega_s I_{dr} - \frac{R_r}{\sigma L_r}I_{qr} - \frac{g\,L_m V_s}{\sigma L_s L_r} + \frac{V_{qr}}{\sigma L_r}\right)\right) \tag{30}$$

where $\sigma = 1-(L_m^2/L_sL_r)$ is the leakage factor, and $g$ is the slip of the induction machine. We pose $X = L_mV_s / L_s$ and $Y = \sigma L_r$.

Finally, the stabilizing control law for active power is defined by:

$$V_{qr} = -\frac{2Y}{3X}\dot{P}_s^* + g\,\omega_s Y I_{dr} + R_r I_{qr} + gX - \frac{2Y}{3X}k_1 e_1 \tag{31}$$

To ensure the convergence of the Lyapunov candidate function, replacing expression (31) in (30) gives:

$$\dot{V}(e_1) = -k_1 e_1^2 < 0 \tag{32}$$

where $k_1$ is a positive constant.

**B) Reactive Power Control**

The reactive power error can be given by:

$$e_2 = Q_s^* - Q_s \tag{33}$$

The derivative of (33) is:

$$\dot{e}_2 = \dot{Q}_s^* - \dot{Q}_s \tag{34}$$

Considering $V$ as a Lyapunov candidate function:

$$V(e_2) = \frac{1}{2}e_2^2 \tag{35}$$

The derivative of (35) is given by:

$$\dot{V}(e_2) = e_2\dot{e}_2 = e_2\left(\dot{Q}_s^* - \dot{Q}_s\right) \tag{36}$$

Replacing (22) in (36), we obtain:

$$\dot{V}(e_2) = e_2\left(\dot{Q}_s^* + \frac{3}{2}\frac{L_m}{L_s}V_s\dot{I}_{dr}\right) \tag{37}$$

Such as the derivative of $I_{dr}$ is given by this expression:

$$\dot{I}_{dr} = \frac{dI_{dr}}{dt} = -\frac{R_r}{\sigma L_r}I_{dr} + g\,\omega_s I_{qr} + \frac{V_{dr}}{\sigma L_r} \tag{38}$$

Equation (37) becomes as follows:

$$\dot{V}(e_2) = e_2\left(\dot{Q}_s^* + \frac{3}{2}\frac{L_m}{L_s}V_s\left(-\frac{R_r}{\sigma L_r}I_{dr} + g\,\omega_s I_{qr} + \frac{V_{dr}}{\sigma L_r}\right)\right) \tag{39}$$

Finally, the stabilizing control law for reactive power is defined by:

$$V_{dr} = -\frac{2Y}{3X}\dot{Q}_s^* + R_r I_{dr} - g\,\omega_s Y I_{qr} - \frac{2Y}{3X}k_2 e_2 \tag{40}$$

where $X = L_mV_s / L_s$ and $Y = \sigma L_r$.

To ensure the convergence of the Lyapunov candidate function, replacing expression (40) in (39) gives:

$$\dot{V}(e_2) = -k_2 e_2^2 < 0 \tag{41}$$

With $k_2$ is a positive constant.

## 5 Simulation Results

The backstepping control scheme of the DFIG applied to the rotor side converter (RSC) is represented in Fig. 7.

In this section, the proposed control strategy of 1.5MW DFIG (see appendix) is tested by simulation by using MATLAB/Simulink software. As a result, several simulation tests were performed; their goals are the control of active and reactive power at the stator side of the DFIG through its rotor side converter.

Two types of tests were carried out to the wind system illustrated in Fig. 7 to observe the effectiveness of the backstepping technique for different operating conditions [19]:

1. References tracking test at variable wind speed with MPPT technique and for unity power factor.
2. Robustness test against the variations of the parameters of the DFIG at fixed wind speed.

The first test is shown in Fig. 8; it was performed with a variable wind speed presented in Fig. 2. The stator active power of DFIG follows its reference perfectly (Fig. 8(a)), which corresponding to the variable wind turbine power extracted by the MPPT algorithm, while the reactive power reference is fixed to zero (Fig. 8(b)) to keep a unit power factor at the grid side of the DFIG.

The analysis of the simulation results of Fig. 8 shows a good reference tracking for the active and reactive power with fast response time and without overshoot.

To test the robustness of the backstepping control technique of the DFIG, we also studied the effect of parametric changes of the generator on the performances of this last control strategy. To realize this test we increase the rotor resistance ($R_r$) by 100% of its nominal value (case of warming-up of rotor windings) and decrease the mutual inductance ($L_m$) by 50% of its nominal value (case of inductances saturation). Fig. 9 shows the simulation results of this test, it has shown the active power, the reactive power, the rotor current, and the stator current response respectively of the DFIG. In this test the wind turbine is driven from the sub-synchronous to the super-synchronous speed, going through the synchronous speed.

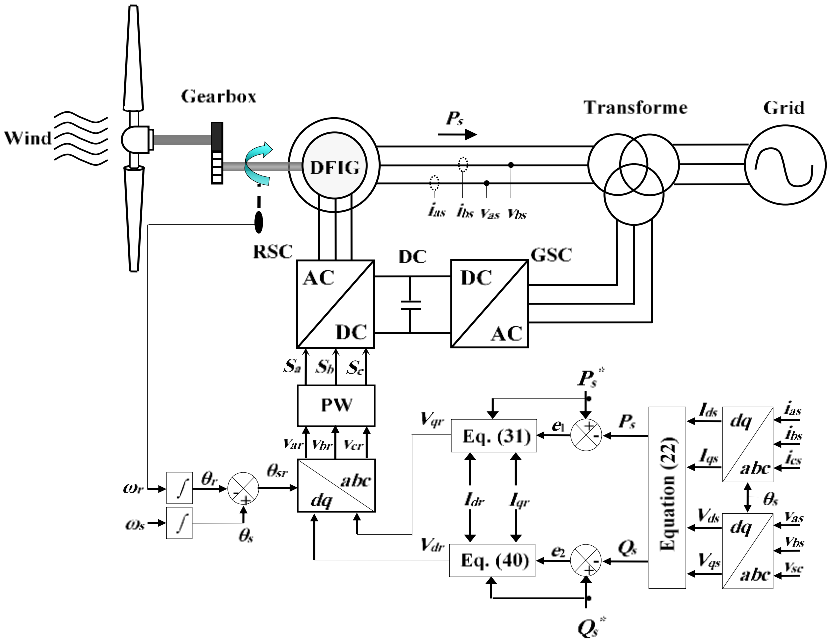


**Fig. 7** Schematic diagram of the backstepping control method for DFIG.

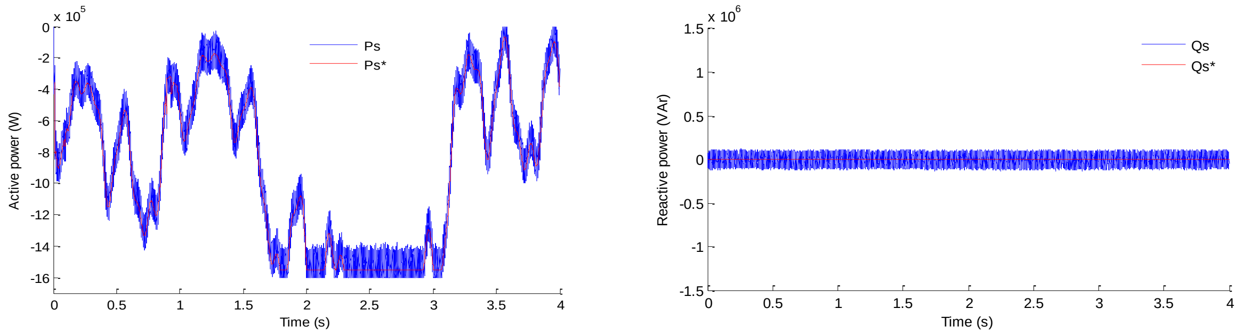


(a) (b)

**Fig. 8** Simulation results of the backstepping control of DFIG at variable wind speed; a) active power response and b) reactive power response

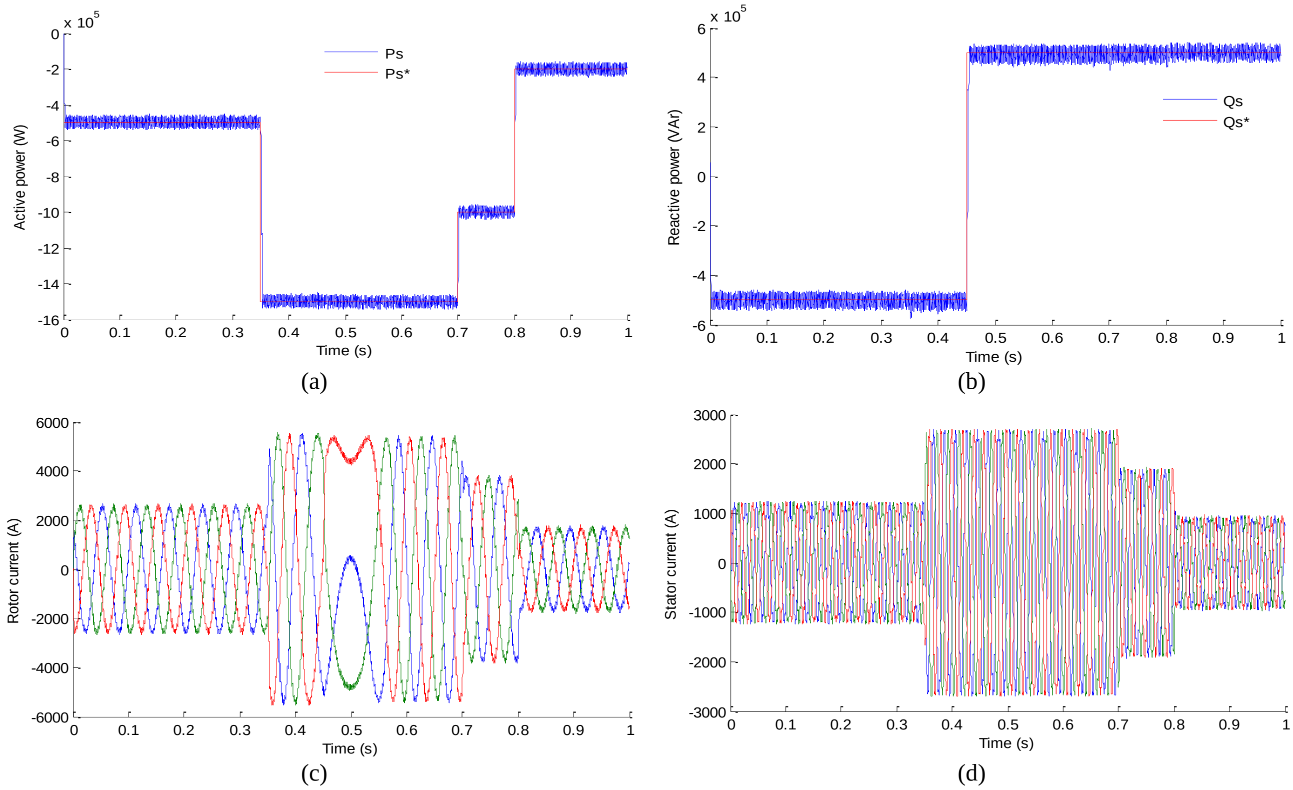


**Fig. 9** Simulation results of the robustness test against parameters variations of DFIG for the backstepping control; a) active power response, b) reactive power response, c) rotor current response, and d) stator current response.

Simulation results in Fig. 9 show the robustness of the backstepping control strategy against parameters variations of the DFIG, unlike for the vector control strategy (FOC) based PI (Proportional-Integral) controllers [4, 5].

## 7 Conclusion

This paper has presented a nonlinear and a robust control strategy of the doubly fed induction generator (DFIG) applied in a wind energy system (WES) by using the backstepping technique.

The first part of this article is intended for the mathematical modeling of WES chain such as the wind speed, the wind turbine, the MPPT technique, and the DFIG model. The second part presents the design of the backstepping controller, this technique ensures a global asymptotic stability via the Lyapunov control function. This control is developed by determining the direct and quadrature components of the rotor voltage applied by the rotor-side converter (RSC).

Simulation results of the backstepping control strategy show high performances and robustness against parameters variations of the DFIG in a wide range of speed, which allows operation of the WES at the maximum of the electrical power produced to the grid with a unit power factor.

## Appendix

**Table 1** Wind turbine parameters.

| Parameter | Rated Value | Unit |
|---|---|---|
| Rated power, $P_n$ | 1.5 | MW |
| Blade radius, $R$ | 35.25 | m |
| Number of blades | 3 | - |
| Gearbox ratio, $G$ | 90 | - |
| Total moment of inertia, $J$ | 1000 | kg.m$^2$ |
| Viscous friction coefficient, $f_r$ | 0.0024 | N.m.s$^{-1}$ |
| Nominal wind speed, $v$ | 12 | m/s |

**Table 2** Doubly fed induction generator parameters.

| Parameter | Rated Value | Unit |
|---|---|---|
| Stator rated voltage, $V_s$ | 398/690 | V |
| Rotor rated voltage, $V_r$ | 225/389 | V |
| Rated current, $I_n$ | 1900 | A |
| Stator rated frequency, $f$ | 50 | Hz |
| Stator inductance, $L_s$ | 0.0137 | H |
| Rotor inductance, $L_r$ | 0.0136 | H |
| Mutual inductance, $L_m$ | 0.0135 | H |
| Stator resistance, $R_s$ | 0.012 | Ω |
| Rotor resistance, $R_r$ | 0.021 | Ω |
| Number of pair of poles, $p$ | 2 | - |
| Slip range, $g$ | -0.3 to 0.3 | - |

**Table 3** Power coefficient $C_p$ parameters.

| $C_1$ | $C_2$ | $C_3$ | $C_4$ | $C_5$ | $C_6$ |
|---|---|---|---|---|---|
| 0.5176 | 116 | 0.4 | 5 | 21 | 0.0068 |

**Table 4** MPPT Proportional-Integral (PI) controller parameters.

| $K_p$ | $K_i$ |
|---|---|
| $10^7$ | $2.10^5$ |

**Table 5** Backstepping controller parameters.

| $k_1$ | $k_2$ |
|---|---|
| $9.10^4$ | $9.10^4$ |

## References


[1] P. K. Chaurasiya, V. Warudkar, and S. Ahmed, "Wind energy development and policy in India: A review," *Energy Strategy Reviews*, Vol. 24, pp. 342–357, 2019.

[2] J. Bhukya and V. Mahajan, "The controlling of the DFIG based on variable speed wind turbine modeling and simulation," *IEEE 6th International Conference on Power Systems*, 2016.

[3] L. Makhlouf and S. Lassaad, "Steady state analysis of a doubly-fed induction generator," *IEEE International Conference on Green Energy Conversion Systems*, 2017.

[4] Y. Djeriri, A. Meroufel, A. Massoum, and Z. Boudjema, "A comparative study between field oriented control strategy and direct power control strategy for DFIG," *Journal of Electrical Engineering*, Vol. 14, No. 2, pp. 169–178, 2014.

[5] Y. Djeriri, A. Meroufel, and M. Allam, "Artificial neural network-based robust tracking control for doubly fed induction generator used in wind energy conversion systems," *Journal of Advanced Research in Science and Technology*, Vol. 2, No. 1, pp. 173–181, 2015.

[6] F. Z. Belaimeche, A. Bentaallah, S. Massoum, and P. Wira, "A comparative study between a simplified fuzzy PI and classic PI input-output linearizing controller for the wind-turbine doubly fed induction generator," *Elektrotehniski Vestnik/Electrotechnical Review*, Vol. 85, No. 4, pp. 142–148, 2018.

[7] I. Yaichi, A. Semmah, P. Wira, and Y. Djeriri, "Super-twisting sliding mode control of a doubly-fed induction generator based on the SVM strategy," *Periodica Polytechnica Electrical Engineering and Computer Science*, Vol. 63, No. 3, pp. 178–190, 2019.

[8] N. Khemiri, A. Khedher, and M. F. Mimouni, "Wind energy conversion system using DFIG controlled by backstepping and sliding mode strategies," *International Journal of Renewable Energy Research*, Vol. 2, No. 3, pp. 421–434, 2012.

[9] R. Rouabhi, R. Abdessemed, A. Chouder, and A. Djerioui, "Hybrid backstepping control of a doubly fed wind energy induction generator," *The Mediterranean Journal of Measurement and Control*, Vol. 11, No. 1, pp. 367–376, 2015.

[10] Z. Sabiri, N. Machkour, N. Rabbah, M. Nahid, and E. Kheddioui, "Command of a doubly fed induction generator with a backstepping controller for a wind turbine application," *International Review of Automatic Control*, Vol. 10, No. 1, pp. 56–62, 2017.

[11] E. G. Shehata, "Sliding mode direct power control of RSC for DFIGs driven by variable speed wind turbines," *Alexandria Engineering Journal*, Vol. 54, No. 4, pp. 1067–1075, 2015.

[12] Q. Wu and Y. Sun, *modeling and modern control of wind power*. Wiley-IEEE Press, ISBN: 978-1-119-23626-9, Feb. 2018.

[13] M. Loucif, A. Boumediene, and A. Mechernene, "Backstepping control of double fed induction generator driven by wind turbine," *Proceedings of the 3rd International Conference on Systems and Control*, Algiers, Algeria, Oct. 29-31, 2013.

[14] M. Doumi, A. Aissaoui, A. Tahour, M. Abid, and K. Tahir, "Nonlinear integral backstepping control of wind energy conversion system based on a double-fed induction generator," *PRZEGLĄD ELEKTROTECHNICZNY*, Vol. 3, pp. 130–135, 2016.

[15] M. Nadour, A. Essadki, M. Fdaili, and T. Nasser, "Inertial response using backstepping control from DFIG based wind power plant for short-term frequency regulation," *IEEE 6th International Conference on Control, Decision an Information Technologies*, Paris, France, Apr. 23-26, pp. 268–273, 2019.

[16] Y. Ihedrane, C. E. Bekkali, M. E. Ghamrasni, S. Mensou, and B. Bossoufi, "Improved wind system using non-linear power control," *Indonesian Journal of Electrical Engineering and Computer Science*, Vol. 14, No. 3, pp. 1148–1158, 2019.

[17] S. Mensou, A. Essadki, T. Nasser, and B. B. Idrissi, "An efficient nonlinear backstepping controller approach of a wind energy conversion system based on a DFIG," *International Journal of Renewable Energy Research*, Vol. 7. No. 4, pp. 1520–528, 2017.

[18] A. Elmansouri, J. Elmhamdi, and A. Boualouch, "Control by back stepping of the DFIG used in the wind turbine," *International Journal of Emerging Technology and Advanced Engineering*, Vol. 5, No. 2, pp. 472–478, 2015.

[19] E. M. Youness, D. Aziz, E. G. Abdelaziz, B. Jamal, E. O. Najib, Z. Othmane, M. Khalid, B. BOSSOUFI

[20] E. M. Youness, D. Aziz, E. G. Abdelaziz, B. Jamal, E. O. Najib, Z. Othmane, M. Khalid, and B. BOSSOUFI, "Implementation and validation of backstepping control for PMSG wind turbine using dSPACE controller board," *Energy Reports*, Vol. 5, pp. 807–821, 2019.

**Y. Djeriri** was born in Algeria in 1984. He received the Ph.D. degree in Electrical Engineering from the Electrical Engineering Faculty of Djillali Liabes University at Sidi Bel-Abbes, Algeria, in 2015. He is a member of the Intelligent Control & Electrical Power Systems (ICEPS) research laboratory. His research interests are in the field of robust, advanced and intelligent control methods of AC drives associated with power electronic converters for renewable energy applications.

© 2020 by the authors. Licensee IUST, Tehran, Iran. This article is an open access article distributed under the terms and conditions of the Creative Commons Attribution-NonCommercial 4.0 International (CC BY-NC 4.0) license (https://creativecommons.org/licenses/by-nc/4.0/).